

## In-Silico Design, Synthesis and In-Vitro Studies of 4h-Chromene Derivatives as Anti-Cancer Agent

ANJALI RAMESH, JOYAL K J, NANDANA M, IRSHAD N B,  
KRISHNENDHU MOHAN

Triveni Institute of pharmacy, Kechery, Thrissur, Kerala

Corresponding Author: NANCY THOMAS, M PHARM, ASSOCIATE PROFESSOR, Department of  
Pharmaceutical Chemistry

Date of Submission: 01-04-2026

Date of Acceptance: 10-04-2026

### ABSTRACT

Cancer constitutes the main mortality cause in the world. 4H-Chromene derivatives are an attractive template for the identification of potential anticancer agents. In recent years, there has been much interest in this class of compounds and their potential utility as anticancer drugs. Chromene appears as an important structural component in natural compounds like polyphenols, alkaloids, tocopherols, flavonoids, anthocyanins and generated great attention because of their interesting biological activity. Chemically, 4H-Chromene (benzopyran) is a heterocyclic ring system consisting of a benzene ring fused to a 4H-pyran ring. In this study, we proposed to develop novel series of anticancer agents. The anticancer activity helps to reduce the pain associated with carcinoma. The selected 4-phenyl-4H-Chromene derivatives undergoes *in-silico* molecular modeling studies. In the docking study, ligands are docked against anticancer (EGFR receptor) target using PyRx and Discovery studio visualizer. *In-silico* analysis includes drug-likeness and toxicity parameters was carried out using Geinforce software. Based upon the results obtained from the molecular modeling, the derivative was selected for the synthesis. The synthesis was carried out through the three component one-pot reaction of appropriate substituted benzaldehyde, malononitrile and resorcinol. The synthesised compound was characterized by TLC, IR, Mass, <sup>1</sup>H NMR and <sup>13</sup>C NMR data and screened for their *in-vitro* anticancer activity. The anticancer study was carried out by MTT assay in colorectal cancer (CaCo2) cell line. All the compounds showed significant level of anti-cancer activity compared to the standard reference (Erlotinib). The synthesized compound C4 showed good anti-cancer activity. This study reveals that the compound tends to have good activity against colorectal carcinoma and thereby may reduce the pain related to cancer because of its anti-cancer activity.

**KEY WORDS:** 4H-Chromene Derivatives, Molecular docking, ADMET, Synthesis, Characterization, *In-vitro* study

### I. INTRODUCTION

4H-Chromene and its derivatives are biologically interesting compounds known for their antimicrobial, antifungal [1], antioxidant [2], antileishmanial [3], antitumor [4], hypotensive[5], antiproliferative [6], local anesthetics [7], Antiallergenics[8,9], central nervous system activities and effects [10], as well as treatment of Alzheimer's disease [11] and schizophrenia disorder [12]. Fused Chromene ring systems have platelet anti-aggregation, local anesthetics [13,14,15] and antihistaminic activities[16]. They also exhibit antidepressant effect[17], inhibitory effect on influenza virus sialidases [18,19], DNA breaking activities and mutagenicity [20], antiviral activities [21].

4H-Chromene are generally prepared by one-pot synthesis using different 2-benzylidene malononitriles and substituted resorcinol in the presence of methanol and calcium hydroxide at room temperature [22]. In addition, the reported methods consist of the condensation of resorcinol, aryl aldehyde and malononitrile in the presence of diethylamine under reflux using ethanol as a solvent or 2-aminopyridine as an efficient organo-base-catalyst [23].

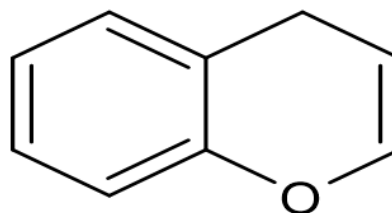


Figure 1: 4H-CHROMENE

**4H-Chromene based drugs that are currently in clinical trials**

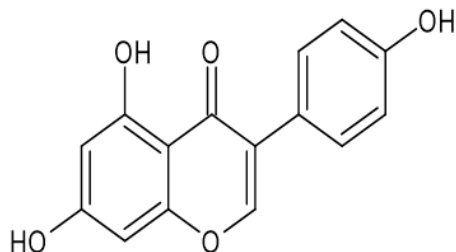


Figure 2: GENISTEIN

Activity: anticancer properties [24], anti-inflammatory property [25].

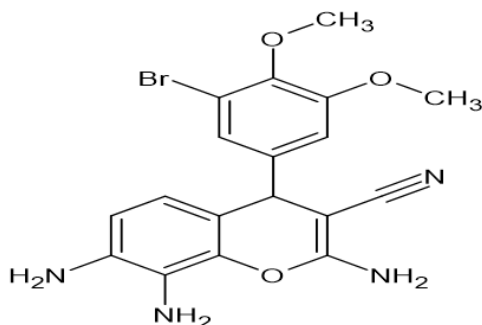


Figure 3: CROLIBULIN

Activity: potent microtubule-targeting agent [26].

### COLORECTAL CANCER

Cancer is a group of disease characterized by the uncontrolled growth and spread of abnormal cells. Colorectal cancer is one of the most commonly diagnosed cancer and the second cause of cancer related death in worldwide. It originates in the colon or in the rectum by the abnormal growth of cells that form a polyp. The polyp form and appear in the epithelial tissue that lines the colon or rectum.

There are four stages of colorectal cancer

- Stage I
- Stage II
- Stage III
- Stage IV

The tumor severity with stage 1 being the least malignant. And the stage 4 being the most malignant [27].

### Pathophysiology

The progression from normal colonic epithelium to dysplasia and eventually carcinoma occurs due to genetic changes that accumulate over time. Colorectal cancer develops mainly through three overlapping genetic pathways:

chromosomal instability (CIN), mismatch repair deficiency (MMR), and CpG island methylator phenotype (CIMP) [28].

The CIN pathway, also known as the classical adenoma–carcinoma sequence, involves an imbalance between oncogenes and tumor-suppressor genes due to accumulated mutations. Commonly affected genes include APC, KRAS, and TP53. Mutations in APC, found in about 60% of colorectal cancers, disrupt the Wnt/ $\beta$ -catenin signaling pathway, leading to uncontrolled cell growth, reduced apoptosis, and abnormal cell differentiation [29].

The MMR pathway results from mutations in DNA repair genes such as MLH1, MSH2, MSH6, and PMS2, causing errors during DNA replication and leading to microsatellite instability (MSI). While inherited MMR mutations are seen in Lynch syndrome, most MSI-high tumors are sporadic [30].

The CIMP pathway accounts for about 15% of colorectal cancers and is characterized by hypermethylation of CpG islands, which silences tumor-suppressor genes. These cancers often arise from serrated polyps and are commonly associated with KRAS and BRAF mutations. When CIMP occurs together with MSI, the prognosis is generally better [31].

### Signs and Symptoms

- Constipation
- Weakness and fatigue
- Weight loss
- Iron deficiency anemia
- Abdominal pain
- Blood in stool
- Loss of appetite
- Nausea and vomiting [32]

## Treatments

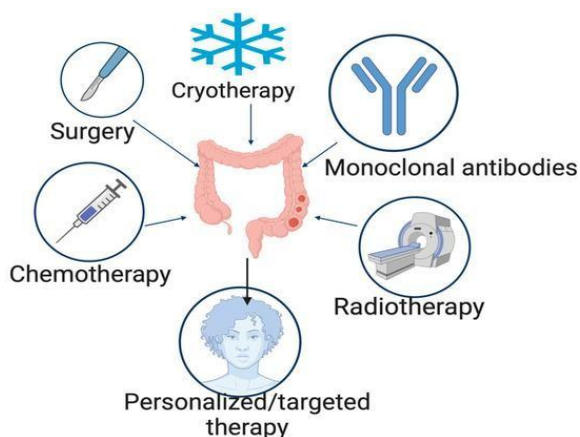


Figure 4: Treatments

- **Surgery**
  - Main treatment for CRC, especially with liver metastasis.
  - Can be done through open or laparoscopic surgery.
  - Common post-surgery complication: infection, thrombosis, adhesion, bowel obstruction, ileus, leakage and ischemia [33].

- **Cryotherapy**

Introduced in 1970s for low rectal cancer. Cryotherapy has been extensively utilized in the treatment of various tumors, particularly in the prostate, kidney, liver and other solid organs [34].

In recent times, cryoablation has been considered a significant approach for treating patient with rectal cancer. Additionally, cryoablation is considered a minimally invasive surgical procedure with low anesthetic requirements. Several factors, such as the tumor site, tumor size, tumor stage and lymph node metastasis, can influence the effectiveness of cryotherapy [35].

- **Radiation therapy**

Radiation therapy has the capability to induce immunogenic cell death, leading to the release of tumor antigens and promote immune cell movement. While radiation therapy is not typically recommended as a routine treatment for colon cancer patients, it may have a role in specific situations. Intraoperative radiation therapy (IORT) is a valuable

technique for increasing the radiation dose in patients with locally advanced primary and recurrent rectal cancer [36].

- **Chemotherapy**

Chemotherapeutic agents used in the treatment of CRC include 5-fluorouracil, irinotecan, oxaliplatin and leucovorin. 5-fluorouracil (5-FU) has been widely used as a first line treatment for cancer for many years, and it is thought to be particularly effective against colorectal cancer. Irinotecan has been found to be effective in treating advanced colorectal cancer that did not respond to treatment with 5-fluorouracil (5-FU) [37].

- **Monoclonal antibodies**

Monoclonal antibodies have gained wide popularity in treatment of colorectal cancer. There are two classes of monoclonal antibodies approved by the FDA for the treatment of CRC; they are vascular endothelial growth factor (VEGF) inhibitor, e.g., bevacizumab and the epidermal growth factor receptor (EGFR) inhibitor, e.g., cetuximab and panitumumab [38].

## DRUG DISCOVERY

Drug discovery is the process by which new candidate medications are discovered in the field of medicine, biotechnology and pharmacology [39]. Historically drugs are discovered by identifying the active ingredient from traditional remedies or by discovery. More recently chemical libraries of synthetic small molecules, natural products, or extracts were screened intact cells or whole organisms to identify substance that had a desirable therapeutic effect in a process known as classical pharmacology [40]. After sequencing of human genomic allowed rapid cloning and synthesis of large quantities of purified proteins, it has become common practice to use high throughput screening of large compounds libraries against isolated biological targets which are hypothesized to be disease modifying in a process known as reverse pharmacology. Hits from these screens are then tested in cells and in animals for efficacy [41]. Modern drug discovery involved the identification of screening hits, medicinal chemistry and optimization of those hits to increase affinity, selectivity, efficacy, and metabolic stability [42]. Once a compound that fulfils all of these requirements has been identified, the process of drug development can continue [43].

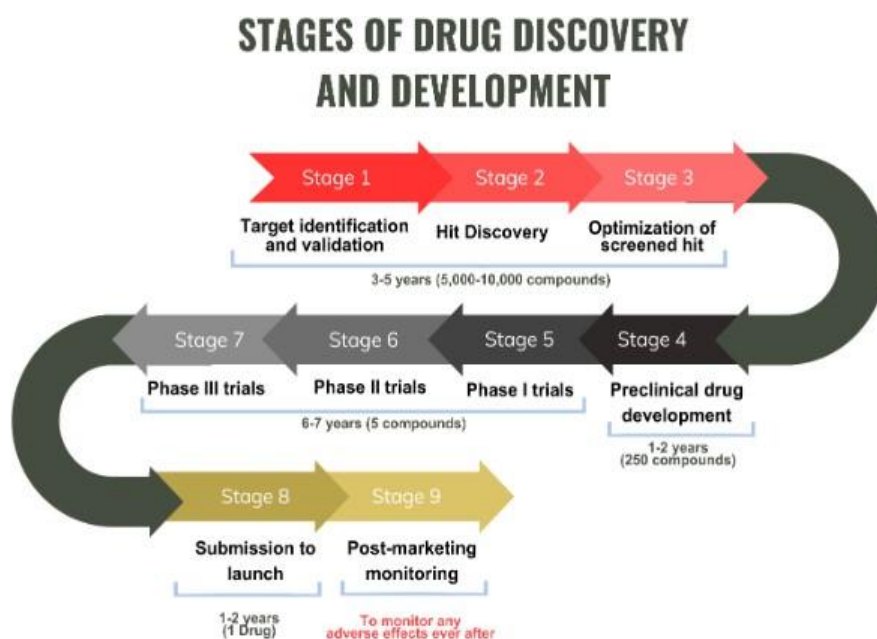


**Figure 5: Stages of drug discovery and development**

Drug discovery begins with target identification, followed by target validation, hit discovery, lead optimization and preclinical/clinical development. Successful drug candidates progress to the development stage, where they undergo clinical trials and submit for approval to launch on the market [44]. Methods used include data-mining, phenotype screening and bioinformatics, potential targets must be validated to determine their rate-limiting role in disease progression or induction. Establishing a strong link between the target and disease builds confidence in the scientific hypothesis, leading to greater success and efficiency in later stages [45]. Compound screening assays are then used to discover novel hit compounds. Strategies include physical methods like mass spectrometry, fragment screening, nuclear magnetic resonance, screening, DNA encoded chemical libraries, high throughput screening and *In-silico* methods like virtual screening. After identifying hit compounds, properties like absorption, distribution, metabolism, excretion and toxicity should be considered and optimized. Unfavourable pharmacokinetic and toxicity profiles can lead to failure in clinical trials. Physical and computational screening techniques are often integrated to

complement each other and maximize screening results [46].

#### STRUCTURE CONSTRUCTION SOFTWARE ChemsSketch

It facilitates the creation and alteration of chemical structure images with various tools for drawing and editing. It supports the visualization of molecules in both two and three dimensions, allowing users to understand chemical bond structures and functional groups. Chem3D, another product from Advanced Chemistry Development laboratories this by providing advanced visualization capabilities such as molecular rotation and colour application, which enhance the clarity of chemical models. It includes multiple templates for ions and functional groups and offers tools for adding text and optimizing models [47].

## II. MATERIALS AND METHODS

### *In-Silico* Molecular Modeling

Molecular modeling is a tool for the discovery of new drugs for various diseases by the help of computational methods.

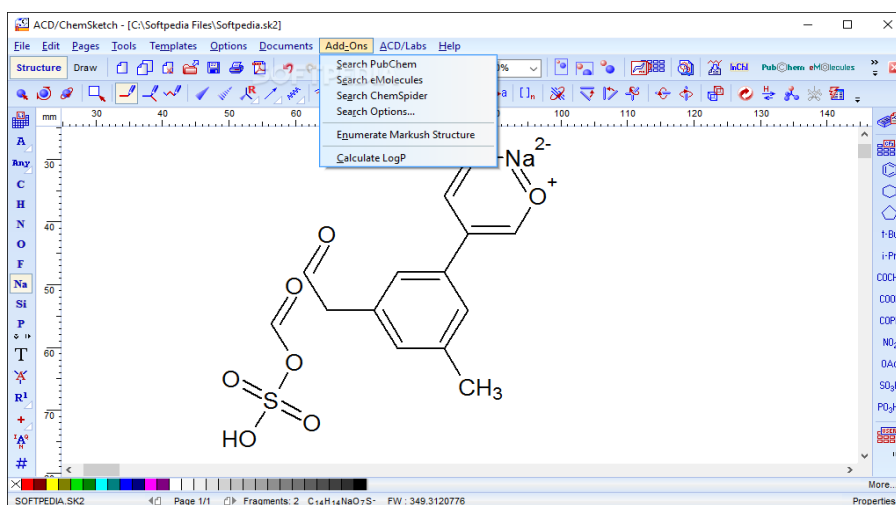


Figure 6: Chemsketch

#### Softwares used

Chemsketch, Geinforce, ForceADME, PyRx and Discovery studio visualizer.

#### Methodology of molecular docking

##### Ligand designing and optimization

From the literature review, molecules called 4*H*-Chromene were chosen for the further study. 10 ligands were designed by giving different substitution at 4th and 7th position of 4*H*-Chromene. The molecular structure and 3D structure are drawn by using the software chemsketch. The selected ligands were optimized by calculating the lipophilicity, molecular weight, sizes and shape of the ligand.

##### Analysis of Lipinski rule of five

Lipinski rule of five was analysed by using Molinspiration online software. Open the Molinspiration homepage. Click calculation of molecular properties of Drug-likeness. Draw the required structures in JME window. Click and calculate the properties. Save the properties.

##### Determination of parameters

Drug development involves assessment of absorption, distribution, metabolism and excretion. They are determined by using ForceADME. The program required 2D molecular structural information in ForceADME submission page. Molecules can be directly passed or typed in SMILES format or inserted through molecular sketcher. When the list of molecules is ready to be submitted, the user can start the calculations by clicking on the "Run" button. The output panels are located in the same webpage. There is one panel compiling all the values for each molecules computed parameter values are grouped in the different sections of the on-panel-per-molecule output. The program used the molecular

description values to generate estimates for each of ADME properties then calculates the properties.

##### Target identification and retrieval

Crystallographic structures of the target of interest were obtained from Protein Data Bank (PDB) and saved in standard 3D coordinate format.

TARGETS	PDB ID
EPIDERMAL GROWTH FACTOR RECEPTOR	4HJO

Table 1: Selected target and its PDB ID

Epidermal growth factor receptor is overexpressed or deregulated in many human cancer types, including CRC. A high EGFR expression level has been related to a poor prognosis [48,49]. Targeting EGFR might be a rational approach to treat CRC patients. Erlotinib is a highly potent reversible inhibitor of the tyrosine kinase domain of EGFR. It is an oral compound that is active against a wide range of colon cancers in-vitro [50]. Erlotinib as a monotherapy has also shown activity in metastatic CRC patients, providing a basis for further studies in phase II in combination with chemotherapy.

The epidermal growth factor receptor (EGFR) and its downstream signaling pathways regulate key cellular events that drive the progression of many neoplasms. EGFR is expressed in a variety of human tumors, including gliomas and carcinomas of the lung, colon, head and neck, pancreas, breast, ovary, bladder, and kidney[51].

##### Active site identification

Identification of active sites is crucial in the process of drug discovery. The 3D structure of the enzyme is analysed to identify active site residues and design

drugs which can fit into them. All the targets were possessing natural ligand and so active site residue identification was carried out taking advantage of the same. A protein was loaded in Discovery studio visualizer. A protein which has many chains was cleaned and a single chain of interest was selected. All the residues surrounding this ligand were identified and selected. These molecules were checked in previous literature to confirm its presence in the binding pocket. The same procedure was carried out for all the targets.

#### Preparation of active site

Explicit Hydrogen atoms missing in the PDB structure was added using Discovery studio visualizer. Furthermore, the atom list of the molecules were prepared, which represents numbers of all atoms of the active site residue involved.

#### Energy minimization

Hydrogen added clean files of protein were loaded in online software, PyRx AutoDock vina. PyRx is a virtual screening software for Computational Drug Discovery that can be used to screen libraries of compounds against potential drug targets. It includes

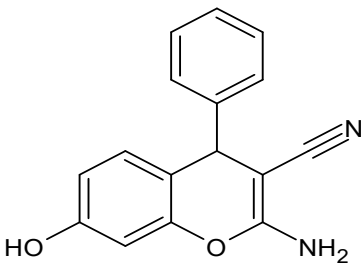
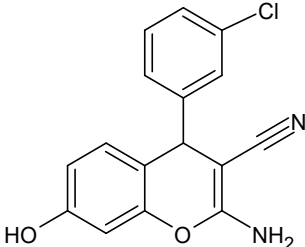
docking wizard with an easy to use, chemical spreadsheet-like functionality and powerful visualization engine that are essential for structure-based drug design. It performs rapid energy minimization of protein molecules using molecular dynamics with all atom representation for each residue in the protein. The conformations and energy states of the newly added hydrogen were fixed and corrected by minimizing the energy.

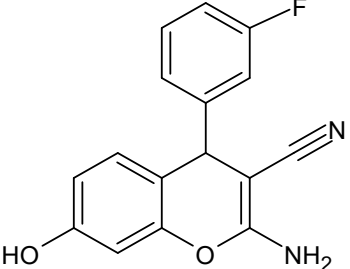
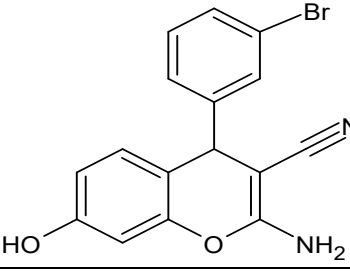
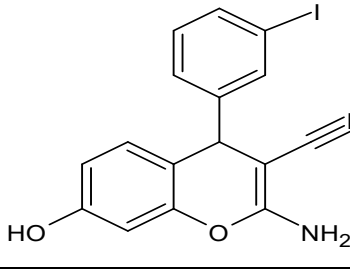
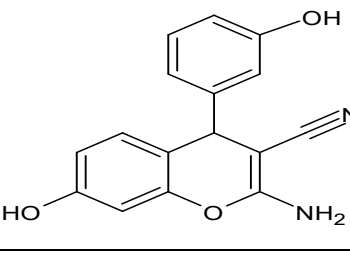
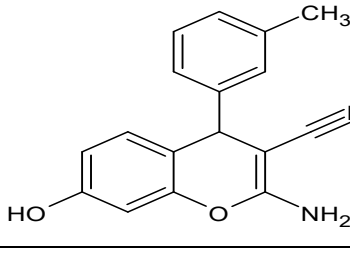
#### Molecular Docking

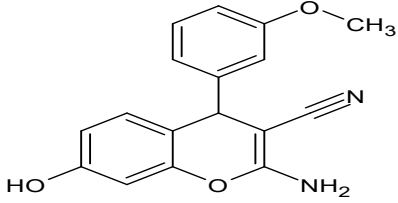
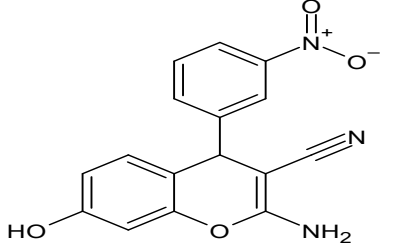
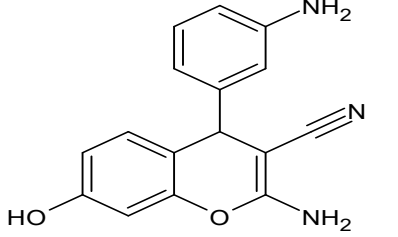
Docking studies were performed using PyRx AutoDock Vina. Docking steps are involved by Download PyRx software. Load protein and ligand files. Convert files to PDBQT format. Define docking grid box around active site. Run docking calculations and binding affinity values obtained(kcal/mol). More negative values can be better binding affinity. Docked complexes were analyzed using Discovery Studio Visualizer.

#### Visual inspection

The structures of each candidates against the target were visualized and the inspected for their goodness of fit or orientation inside the active site.

SL NO	COMPOUND CODE	STRUCTURE	CHEMICAL NAME
1	C1		2-amino-4-phenyl-7-hydroxy-4H-chromene-3-carbonitrile
2	C2		2-amino-4-(2-chlorophenyl)-7-hydroxy-4H-chromene-3-carbonitrile

3	C3		2-amino-7-hydroxy-4-(2-fluorophenyl)-4 <i>H</i> -chromene-3-carbonitrile
4	C4		2-amino-7-hydroxy-4-(2-bromophenyl)-4 <i>H</i> -chromene-3-carbonitrile
5	C5		2-amino-7-hydroxy-4-(2-iodophenyl)-4 <i>H</i> -chromene-3-carbonitrile
6	C6		2-amino-4-(3-hydroxyphenyl)-7-hydroxy-4 <i>H</i> -chromene-3-carbonitrile
7	C7		2-amino-7-hydroxy-4-(2-methylphenyl)-4 <i>H</i> -chromene-3-carbonitrile

8	C8		2-amino-7-hydroxy-4-(3-methoxyphenyl)-4 <i>H</i> -chromene-3-carbonitrile
9	C9		2-amino-7-hydroxy-4-(3-nitrophenyl)-4 <i>H</i> -chromene-3-carbonitrile
10	C10		2-amino-4-(3-aminophenyl)-7-hydroxy-4 <i>H</i> -chromene-3-carbonitrile

**Table 2: Compounds undergoing docking study**

Targeted analogues are shown in the table 3.

SL NO	COMPOUNDS	R1	R2
1	C1	H	OH
2	C2	Cl	OH
3	C3	F	OH
4	C4	Br	OH
5	C5	I	OH
6	C6	OH	OH
7	C7	CH <sub>3</sub>	OH
8	C8	OCH <sub>3</sub>	OH

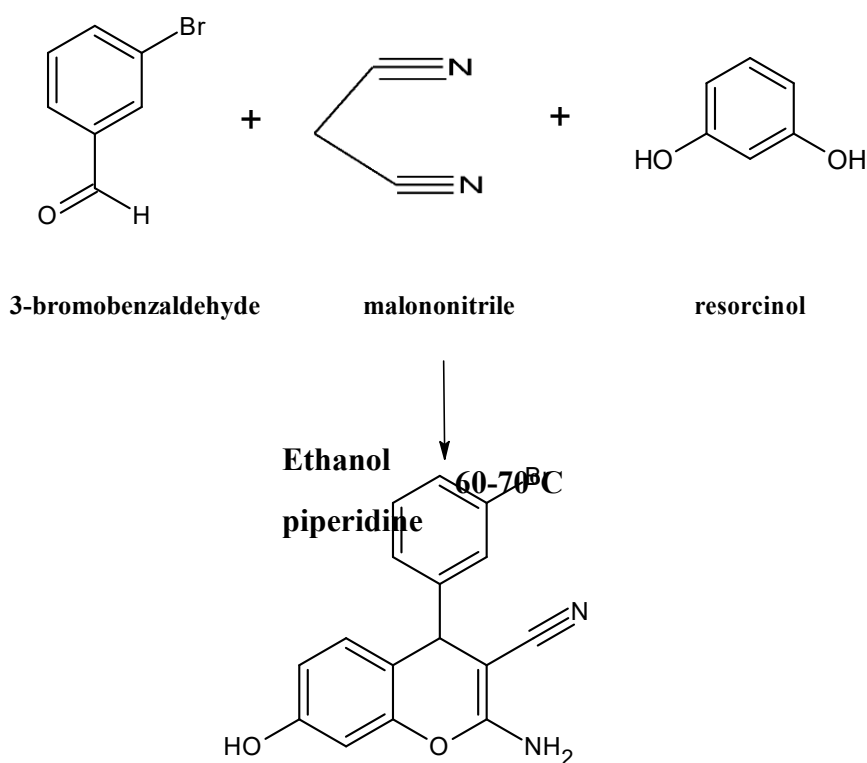
9	C9	NO <sub>2</sub>	OH
10	C10	NH <sub>2</sub>	OH

**Table 3: Targeted analogues**

### Synthesis OF 2-Amino-7-Hydroxy-4-(3-Bromophenyl)-4H-Chromene-3-Carbonitrile

#### Procedure

A mixture of substituted benzaldehyde(1mmol), malononitrile(1mmol), resorcinol(1mmol) were combined in ethanol(15ml) and piperidine(0.2moleq) as catalyst was added and refluxed at room temperature for 3 hours. After the completion of reaction, the reaction mixture was cooled to room temperature. The precipitated solid was filtered and washed with cold ethanol-water and crystallized from ethanol. The residue purified thin layer chromatography on silica gel using n-hexane\ethyl acetate(7:3) as eluent, resulting in the corresponding 2-amino-7-hydroxy-4-(2-bromophenyl)-4H-chromene-3- carbonitrile [52].



### 2-amino-7-hydroxy-4-(2-bromophenyl)-4H-chromene-3-carbonitrile

**Figure 7: Synthesis of 2-amino-7-hydroxy-4-(3-bromophenyl)-4H-Chromene-3-carbonitrile**

#### Spectral analysis

##### IR spectroscopy

The range of electromagnetic radiation between 0.8 and 500  $\mu\text{m}$  was referred as infrared radiation, which was represented with percent transmittance as the ordinate and the wave number ( $\text{cm}^{-1}$ ) as the abscissa. It was an important record which gives sufficient information about the structure of a compound [53].  
Instrument- bruker IR spectrometer

Model- alpha II

Software- opus

##### NMR spectroscopy

NMR spectroscopy was an important tool for determining the structures of a molecule. NMR spectrum can give almost detailed information about molecular structure. <sup>1</sup>H and <sup>13</sup>C NMR helps to determine the number of proton and carbon atoms present in the molecule. DMSO was used as a solvent

[54].

Instrument- varian NMR spectrometer

Model- 400MHz

Software- VNMRJ

#### Mass spectroscopy

It was the major tool used to determine the molecular mass of the compound and its elimination composition. The ionization method used is electron spray ionization. Mass spectra of the samples were recorded on a Waters e 2695-Waters 3100 instrument with ESI-PMT arrangement as the mode of ionization and type of detector respectively [55].

Instrument- LCMS with PDA and SQ Detector

Model- waters

Software- Mass Lynx

#### In-vitro study

##### Method

The In vitro MTT assay for the test item: 4*H*-Chromene Derivative was performed on CaCo2 cell line to determine the level of cytotoxicity.

##### Preparation of test item for cytotoxicity screening

10mg of test item was weighed and dissolved in DMEM-HG medium supplemented with 2% inactivated FBS to obtain a stock solution of 10 mg/ml. Furthermore, serial-two-fold dilutions were prepared from the stock solution to prepare lower concentrations for cytotoxicity testing.

##### Cell line and culture medium

CaCo-2 cells were procured from NCCS, Pune, India. Stock cells were cultured in DMEM supplemented with 10% inactivated Fetal Bovine Serum (FBS), Penicillin (100 IU/mL), Streptomycin (100 mg/mL) and Amphotericin B (5 mg/mL) in a humidified atmosphere of 5% CO<sub>2</sub> at 37 °C until confluent. The cells were dissociated with TE solution (0.25% Trypsin, 0.02% EDTA in Hank's balanced salt solution). The stock cultures were grown in 25 cm<sup>2</sup> culture flasks and cytotoxicity studies were carried out in 96-well micro-titer plate.

##### Determination of cell cytotoxicity by MTT Assay

The cell culture monolayer was trypsinized and the cell count was adjusted to 100000 cells/mL using

DMEM- HG containing 10 % FBS. To each well of the 96 well microtiter plate, 0.1 mL of the diluted cell suspension was seeded. After 24hrs, when a partial monolayer was formed, the supernatant was flicked off, the monolayer was washed once with DPBS. Then cells were treated with different test concentration varying from 1000 µg/mL to 7.8 µg/ml. The untreated cells were maintained as cell control for comparison. The plates were then incubated at 37 °C for 24hrs in 5% CO<sub>2</sub> incubator and microscopic examination was carried out. After 24hrs, the test solutions in the wells were discarded and 100 µL of MTT diluted with DPBS added to each well. The plate was incubated for 3hrs at 37 °C in 5% CO<sub>2</sub> incubator. The supernatant was removed and 100 µL of DMSO was added to solubilize the formed formazan. The absorbance was measured using a micro plate reader at a wavelength of 570 nm [56].

### III. RESULT AND DISCUSSION

#### IN-SILICO MOLECULAR MODELING

Computational analysis was done to compute ligand protein binding affinity of the compound. The interactions showed efficient docking score which was considered as a good score in ligand-protein interactions. This study explored the action of 4*H*-Chromene derivatives against their target proteins. *In-silico* molecular modeling helped to get the preliminary findings about the lead compound. This information led to develop the useful compounds of simple structure exhibiting anticancer activity and for the treatment of colorectal cancer.

#### In-silico analysis

##### ❖ Drug-likeness assessment

The derived analogues were evaluated for their drug-likeness. It was done by calculating the parameters like Lipinski-rule of 5 and some of their extension parameters like number of rotatable bonds and TPSA. The drug-likeness assessments of the compounds were shown in the following table 4.

SL NO	COMPOUND CODE	MOLECULAR FORMULA	MOLECULAR WEIGHT	NO OF HB A	NO OF HB D	Log p	NO OF ROT. B	TPSA
1	C1	C <sub>16</sub> H <sub>12</sub> N <sub>2</sub> O <sub>2</sub>	264.28	4	2	2.61	1	79.3
2	C2	C <sub>16</sub> H <sub>11</sub> ClN <sub>2</sub> O <sub>2</sub>	298.7	4	2	3.26	1	79.3

3	C3	$C_{16}H_{11}FN_2O_2$	282.27	4	2	2.75	1	79.3
4	C4	$C_{16}H_{11}BrN_2O_2$	343.2	4	2	3.37	1	79.3
5	C5	$C_{16}H_{11}IN_2O_2$	390.2	4	2	3.21	1	79.3
6	C6	$C_{16}H_{12}N_2O_3$	280.28	5	3	2.32	1	99.5
7	C7	$C_{17}H_{14}N_2O_2$	278.3	4	2	2.92	1	79.3
8	C8	$C_{17}H_{14}N_2O_3$	294.3	5	2	2.62	2	88.5
9	C9	$C_{16}H_{13}N_3O_2$	279.3	5	3	2.19	1	105.3
10	C10	$C_{16}H_{11}N_3O_4$	309.3	6	2	2.52	2	122.4

**Table 4: Drug-likeness assessments of 4H-Chromene derivatives**

These results showed that value of all the derivatives were relied within the optimal range. All the compounds have molecular weight less than 500 daltons and possessed number of hydrogen bond donors and hydrogen bond acceptors of all the analogues below 5 and 10 respectively. All the values of partition coefficient and number of rotatable bonds were coming under the limit of 5 and 10.

❖ **ADMET parameters by ForceADME**

ForceADME was a computer software system for predictive modeling of absorption, distribution, metabolism and elimination of chemical substances in the human body. The results for the ADME parameters by means of ForceADME were shown in the table 5.

COMPOUND CODE	ABSORPTION LEVEL	SOLUBILITY LEVEL	METABOLISM	HEPATO TOXICITY
C1	HIGH	MODERATELY SOLUBLE	YES	NO
C2	HIGH	MODERATELY SOLUBLE	YES	NO
C3	HIGH	MODERATELY SOLUBLE	YES	NO

C4	HIGH	MODERATELY SOLUBLE	YES	NO
C5	HIGH	MODERATELY SOLUBLE	YES	NO
C6	HIGH	MODERATELY SOLUBLE	YES	NO
C7	HIGH	MODERATELY SOLUBLE	YES	NO
C8	HIGH	MODERATELY SOLUBLE	YES	NO
C9	HIGH	MODERATELY SOLUBLE	YES	NO
C10	HIGH	MODERATELY SOLUBLE	YES	NO

**Table 5: Result of ADMET parameter**

All the compounds (C1–C10) exhibit high absorption levels, indicating that they are predicted to be efficiently absorbed through the gastrointestinal tract after oral administration. High absorption suggests good permeability and bioavailability, which are essential for effective drug action. The solubility of all compounds is reported as moderately soluble, implying a balanced hydrophilic and lipophilic nature. Moderate solubility is generally acceptable in drug design because extremely low solubility can limit absorption, while excessively high solubility may reduce membrane permeability. Thus, moderate solubility supports optimal drug-like behavior. The metabolism parameter is marked as “Yes” for all compounds, indicating that they are predicted to undergo metabolic transformation in the human body, likely via liver enzymes such as the cytochrome P450 system. Proper metabolic processing is important as it facilitates drug elimination, prevents accumulation and potential toxicity, and supports controlled pharmacological action. Furthermore, all compounds are predicted as “No” for hepatotoxicity, suggesting that they are not

expected to cause liver toxicity. Since the liver is the primary organ responsible for drug metabolism, the absence of hepatotoxicity represents a highly favorable safety parameter in early drug development.

#### Molecular Docking

4H-Chromene derivatives were subjected to molecular docking against epidermal growth factor receptor (EGFR). *In-silico* studies were done by using different softwares like PyRx, ChemsKetch, Geinforce, ForceADME and Discovery studio visualizer. PyRx serves as a primary docking tool. The prepared ligands were validated by docking operation using PyRx and Discovery studio visualizer. The docking score of the ligands were compared with the reference standard.

#### Docking scores of 4H-Chromene derivatives as anticancer agents

The docking score obtained from the preliminary docking program by using PyRx were listed in the table 6.

COMPOUND CODE	DOCKING SCORE
C1	-7.8
C2	-8.2

C3	-7.9
C4	-8.4
C5	-8.0
C6	-7.3
C7	-8.0
C8	-8.2
C9	-8.2
C10	-7.6
<b>STANDARD DRUG (ERLOTINIB)</b>	<b>-7.3</b>

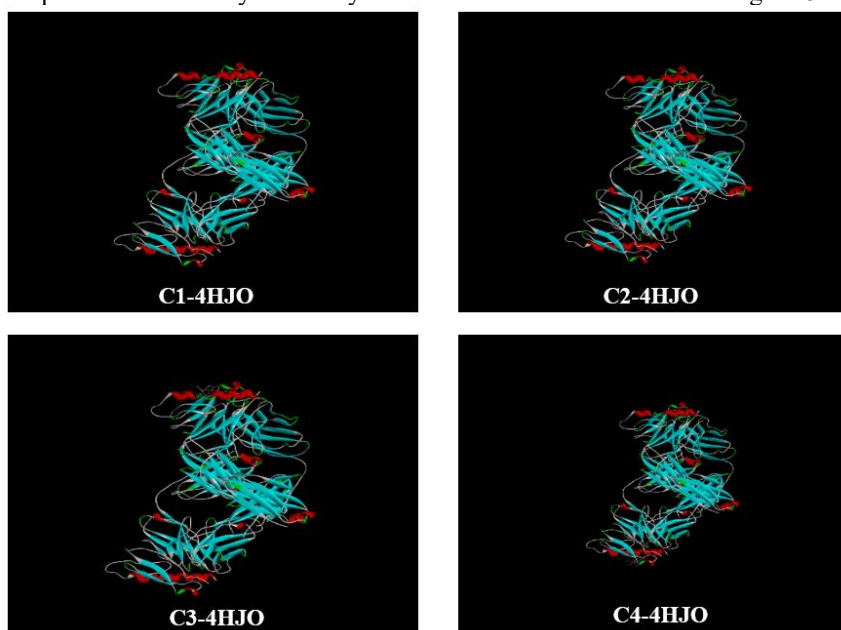
**Table 6: Docking score of 4*H*-Chromene derivatives**

All the compounds were docked against the known target. Epidermal growth factor receptor (EGFR) was the Anticancer protein target. In the case of binding interactions of protein target, all the generated ligands show higher docking score. This can be assured by the pre-screening program of PyRx.

As we go through the docking score of each compound of 4*H*-Chromene derivatives, all the derivatives have equal or higher docking score than

the corresponding standard drug. If we compare the score between the ligands obtained by the combination of 4*H*-Chromene derivatives, the highest score was found to be on C4 (-8.4 kcal/mol). Whereas, the standard drug taken is Erlotinib used for anticancer drug, whose score is (-7.3). Therefore, while we compare the score between C4 and Erlotinib, it seems C4 has more score than Erlotinib. Therefore, C4 is a best compound for the colorectal cancer as per docking score.

Protein-Ligand complex interactions by discovery studio visualizer are shown in the figure 8.



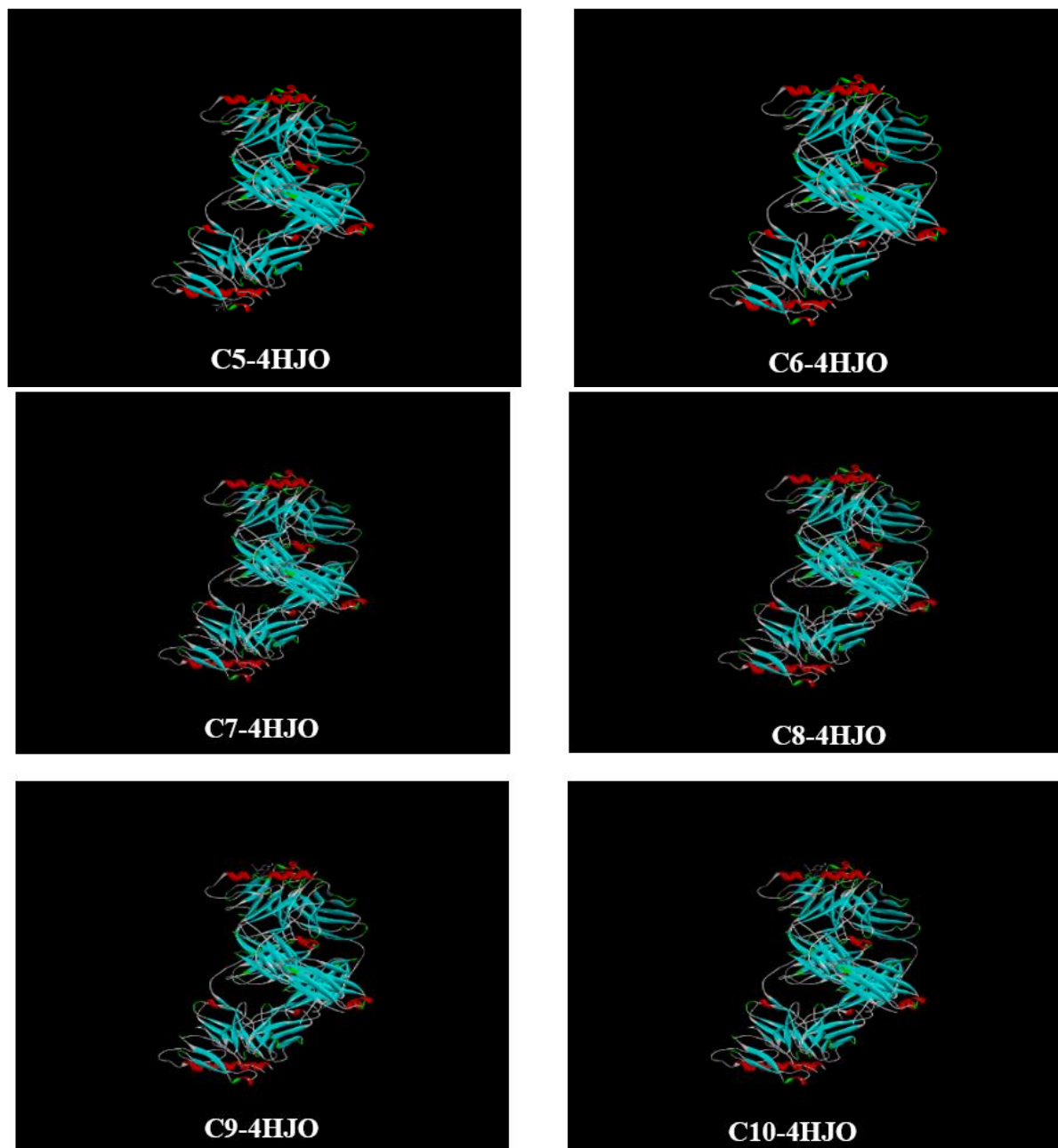
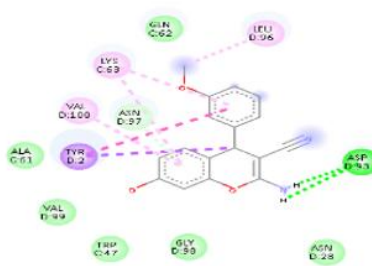
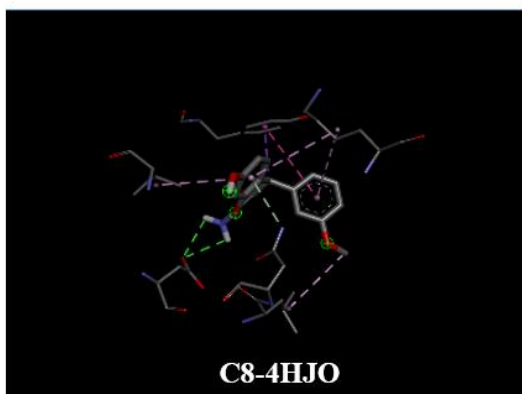
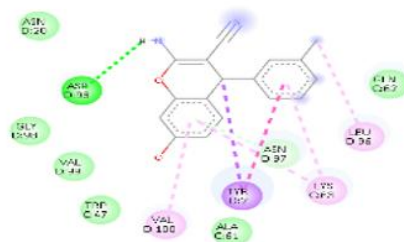
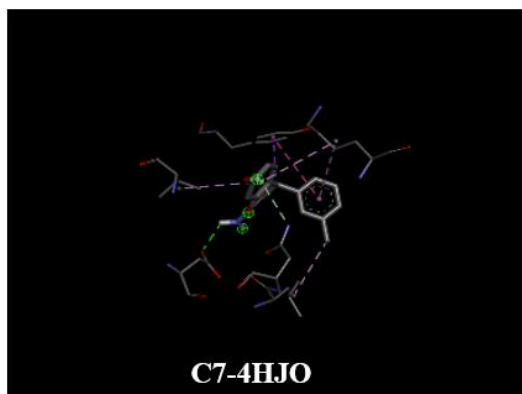
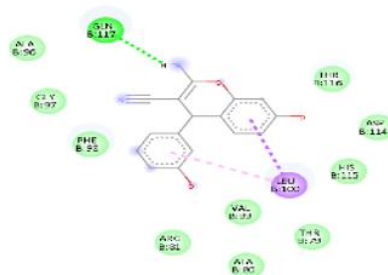
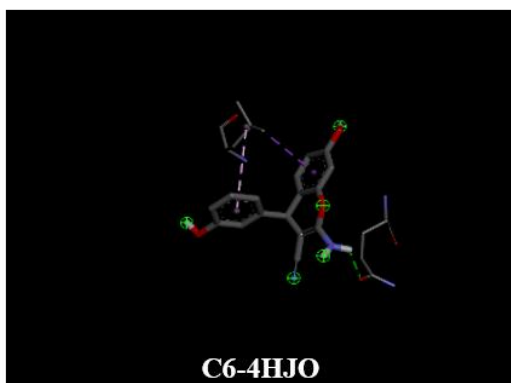
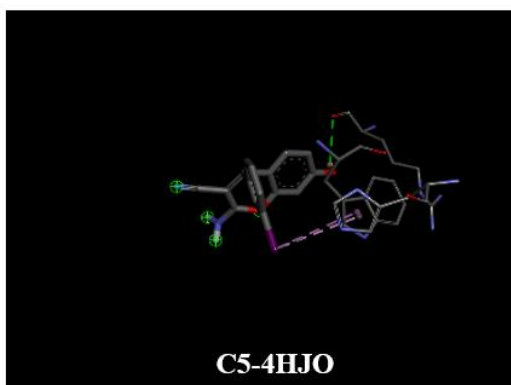


Figure 8: Protein-Ligand complex interaction by Discovery studio visualizer

3D and 2D structure of Ligand-Protein complex interaction by discovery studio visualizer are shown in the figure 9.





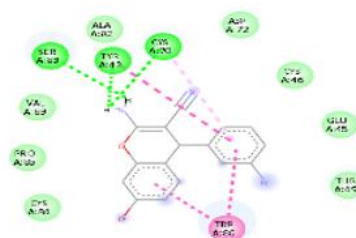
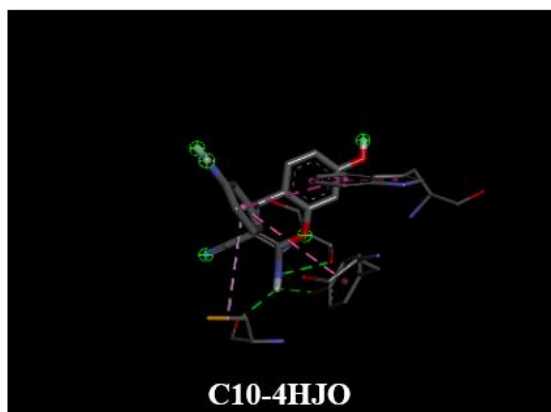
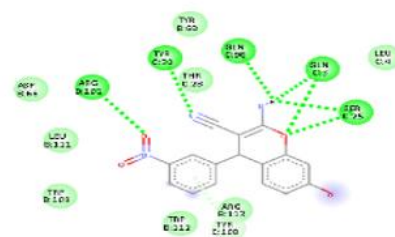
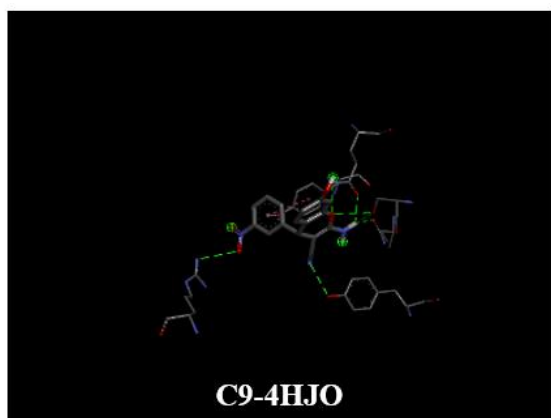


Figure 8: 3D and 2D structure of Ligand-Protein complex interaction by discovery studio visualizer

Ligand-Target hydrogen bond interactions by discovery studio visualizer are shown in the table 7.

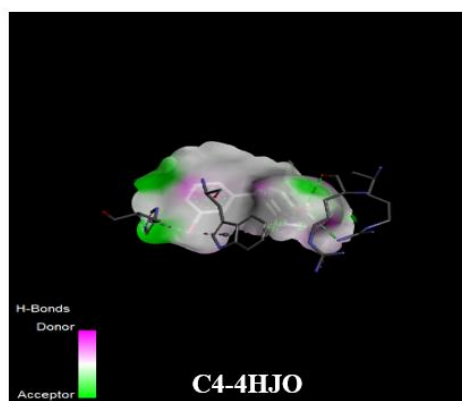
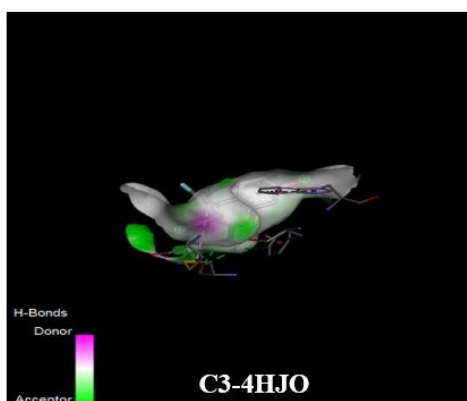
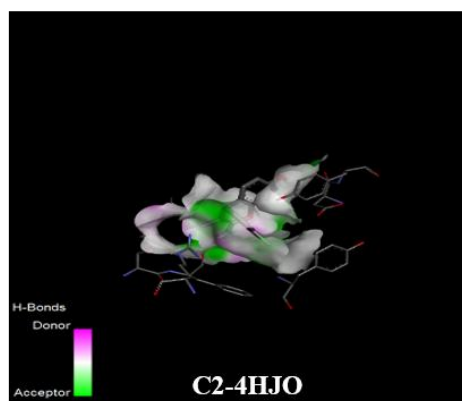
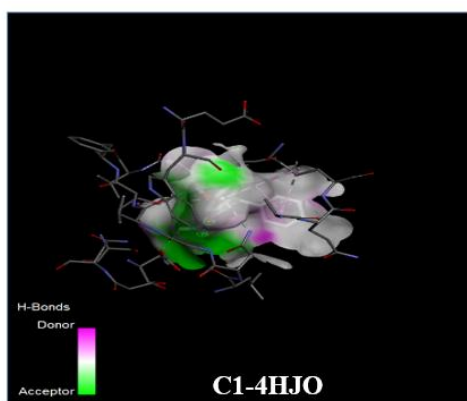
SL NO	COMPOUND CODE	HYDROGEN BOND INTERACTION OF 4HJO
1	C1	ASP:93 VAL:99
C	C2	SER:64 PHE:65
3	C3	TYR:42 CYS:70
4	C4	ARG:38 ARG:41
5	C5	ARG:38
6	C6	GLN:117
7	C7	ASP:93
8	C8	ASP:93

9	C9	GLN:3 SER:25 TYR:32 GLN:98 ARG:101
10	C10	TYR:42 CYS:70 SER:83

**Table 7: Protein-ligand hydrogen bond interactions**

The table summarizes the hydrogen bond interactions between ligands C1–C10 and the amino acid residues of the target protein 4HJO as analyzed using Discovery Studio Visualizer. Hydrogen bonds play a crucial role in stabilizing the ligand within the active site and significantly contribute to binding affinity. Ligand C1 forms hydrogen bonds with ASP-93 and VAL-99, indicating good interaction with both acidic and hydrophobic regions of the protein. C2 interacts with SER-64 and PHE-65, showing bonding with polar and aromatic residues. C3 binds with TYR-42 and CYS-70, suggesting the involvement of aromatic and sulfur-containing residues. C4 forms hydrogen bonds with ARG-38 and ARG-41, reflecting strong

interactions with positively charged residues, while C5 shows a single hydrogen bond with ARG-38, a key basic residue. C6 binds with GLN-117, indicating interaction with a polar residue. Both C7 and C8 form hydrogen bonds with ASP-93, confirming this residue as an important binding site in the active pocket. C9 exhibits multiple hydrogen bond interactions with GLN-3, SER-25, TYR-32, GLN-98, and ARG-101, suggesting that this compound has the strongest and most stable binding among all ligands. Finally, C10 interacts with TYR-42, CYS-70, and SER-83, showing multiple hydrogen bonds and indicating good binding affinity.



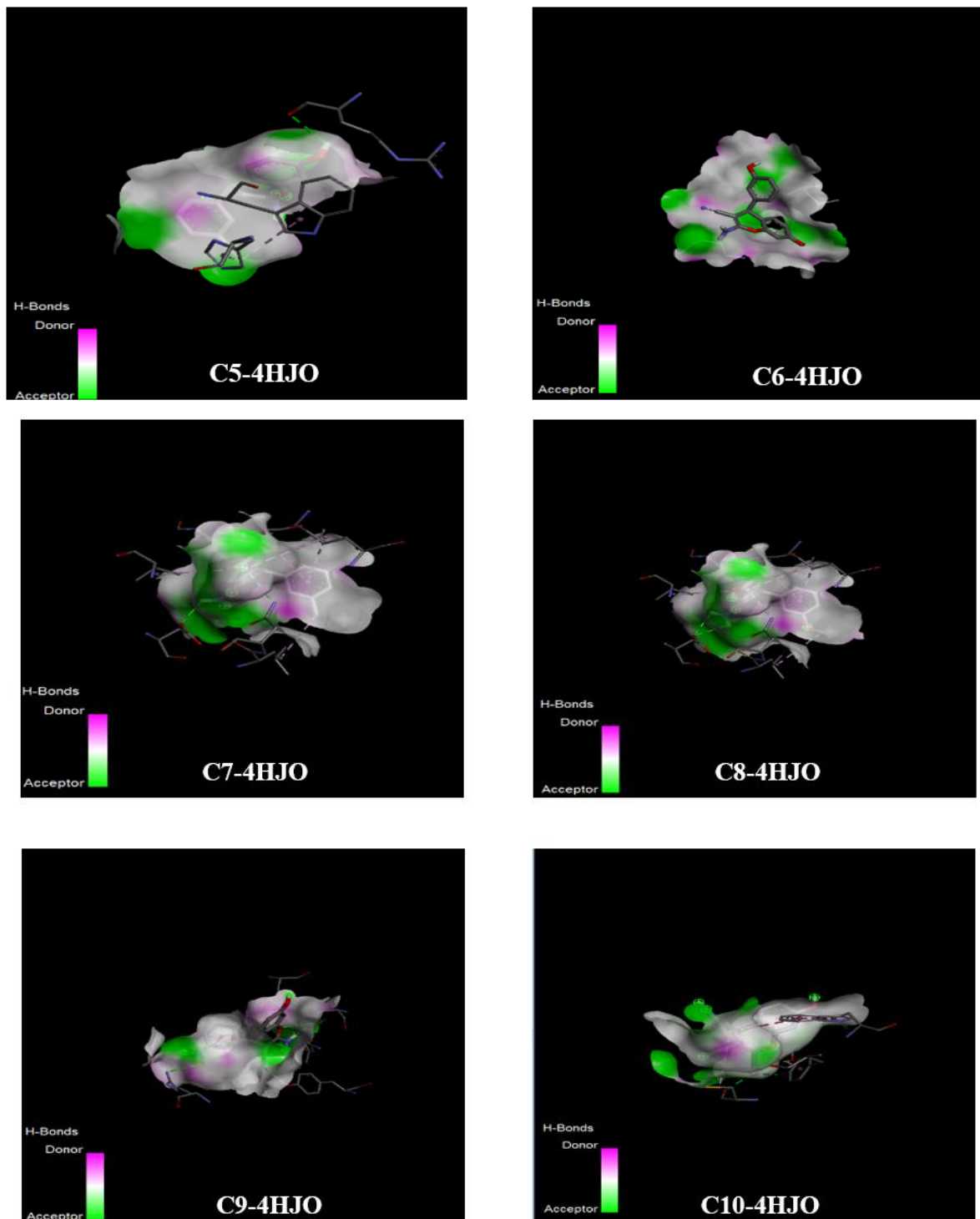


Figure 9: Protein-ligand hydrogen bond interactions

#### Synthesis of 4-phenyl-4*H*-Chromene derivative

Ten 4-phenyl-4*H*-chromene analogues screened by in silico molecular docking and analysis

shows compound C4 has excellent binding affinity against the selected anticancer targets. One of the strategy for the synthesis of these derivative based on

the Knoevenagel condensation and Michael's addition. Malononitrile and benzaldehyde reacted through the Knoevenagel condensation and the corresponding intermediate was then reacted with activated phenol by Michael's addition to get the product, which reacts under the presence of base. The purified residue is subjected to thin layer chromatography on silica gel using n-hexane/ethyl acetate (7:3) as eluent.

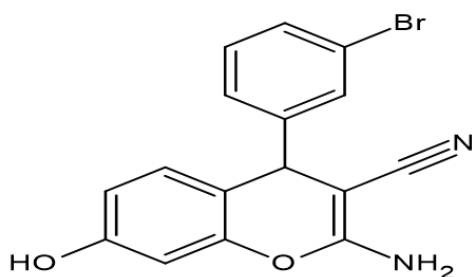


**Figure 10: 2-amino-7-hydroxy-4-(3-bromophenyl)-4H-chromene-3-carbonitrile**

#### Characterization of prepared compound

- Molecular formula: C<sub>16</sub>H<sub>11</sub>BrN<sub>2</sub>O<sub>2</sub>
- Melting point: 108-109°C
- R<sub>f</sub> value: 0.26 (30% EtOAc/Hexane)
- Molecular weight: 343.18g/mol
- Percentage yield: 76.4%

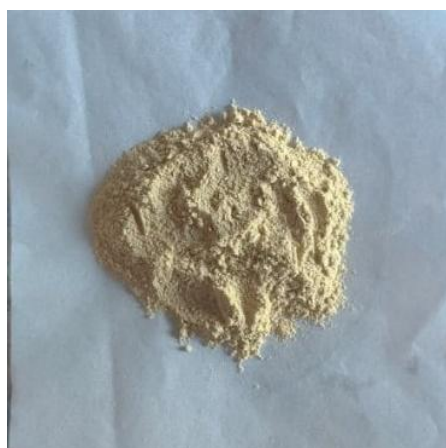


**Figure 11: Synthesized product**

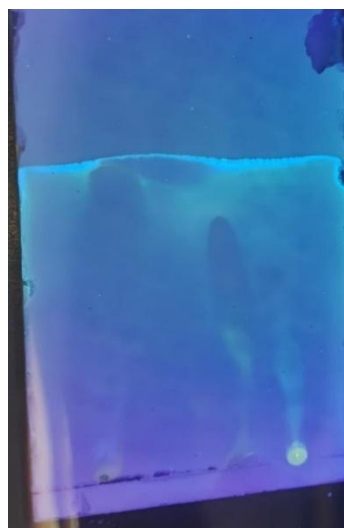
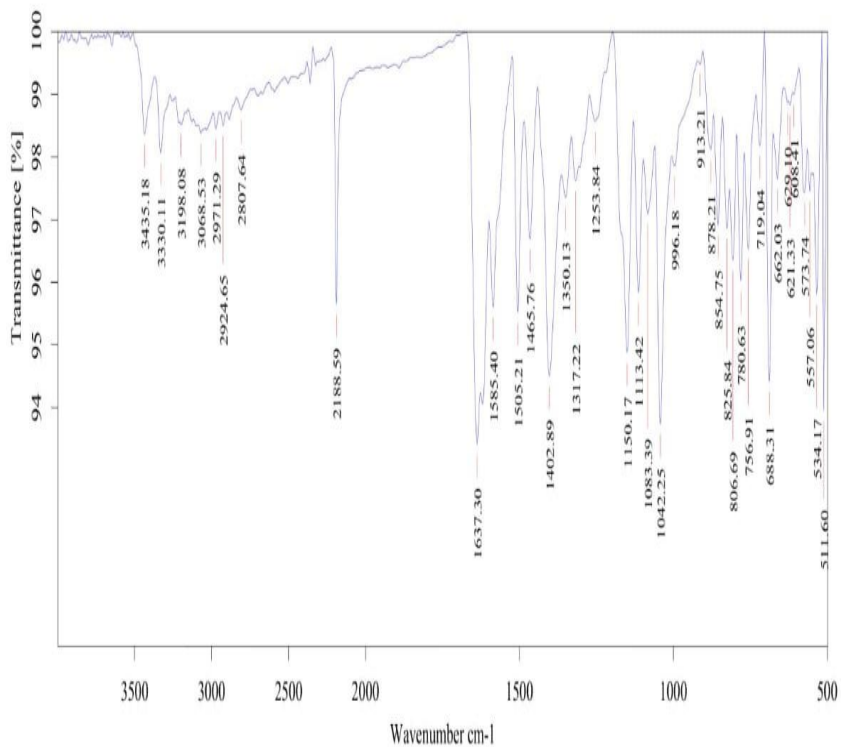


**Figure 12: Thin layer chromatography**

#### ❖ IR spectroscopy

IR (Br): 3435.18(-OH str.), 3330.11(N-H str.), 3068.53(arom-CH str.), 2188.59(CN str.), 1637.30(N-H bending), 1585.40-1402.89(C=C ring str.), 1317.22(C-O str. Of chromene), 1150.17(C-OH str.), 996.18-756.91(arom. CH out plane bending), 534.17(C-Br)cm<sup>-1</sup>.

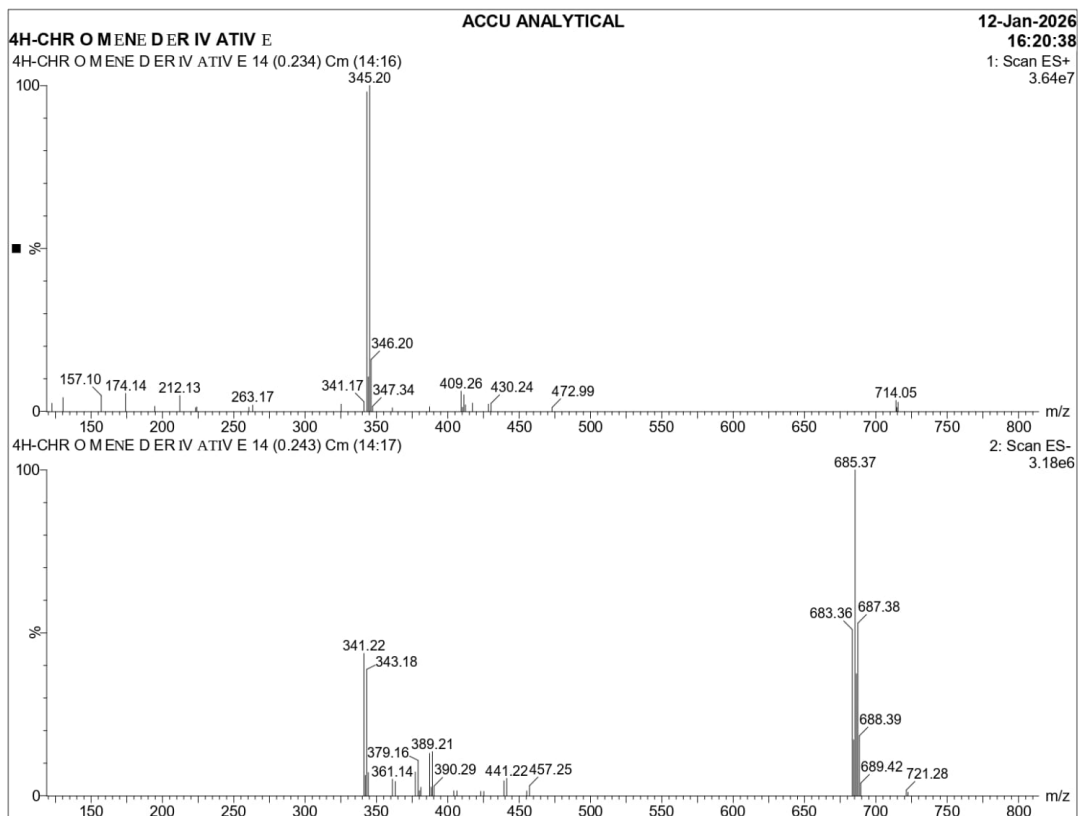
IR spectral data showed two bands for N-H stretching of primary amine group in the range between 3435.18-2188.59cm<sup>-1</sup> amino group was formed. That's why it was used to confirm the formation of compound.



**Graph 1: Graphical representation of IR Spectroscopy**

❖ **MASS Spectroscopy**

ESI MS (ES<sup>+</sup>) (m/z relative abundance) 345.20 M/2 (M+H), 346.20(M+1H), 347.34(M+2H), ESI MS (ES<sup>-</sup>) 341.22(M-H), 343.18[(C<sub>16</sub>H<sub>11</sub>BrN<sub>2</sub>O<sub>2</sub>)], 379.16(M+Na<sup>+</sup>), 361.14(M+NH<sub>4</sub><sup>+</sup>), 390.29(M+K<sup>+</sup>), 687.38(2M+H<sup>+</sup>)  
 The mass indicates the molecular weight of compound. The compound were shown in their (M+H)<sup>+</sup> from except C4 which was shown in the (M-H)<sup>-</sup> form. Mass spectrum of C4 was done in the negative ion mode. The spectral data clearly suggest the formation of expected 4-phenyl-4H-Chromene analogue.



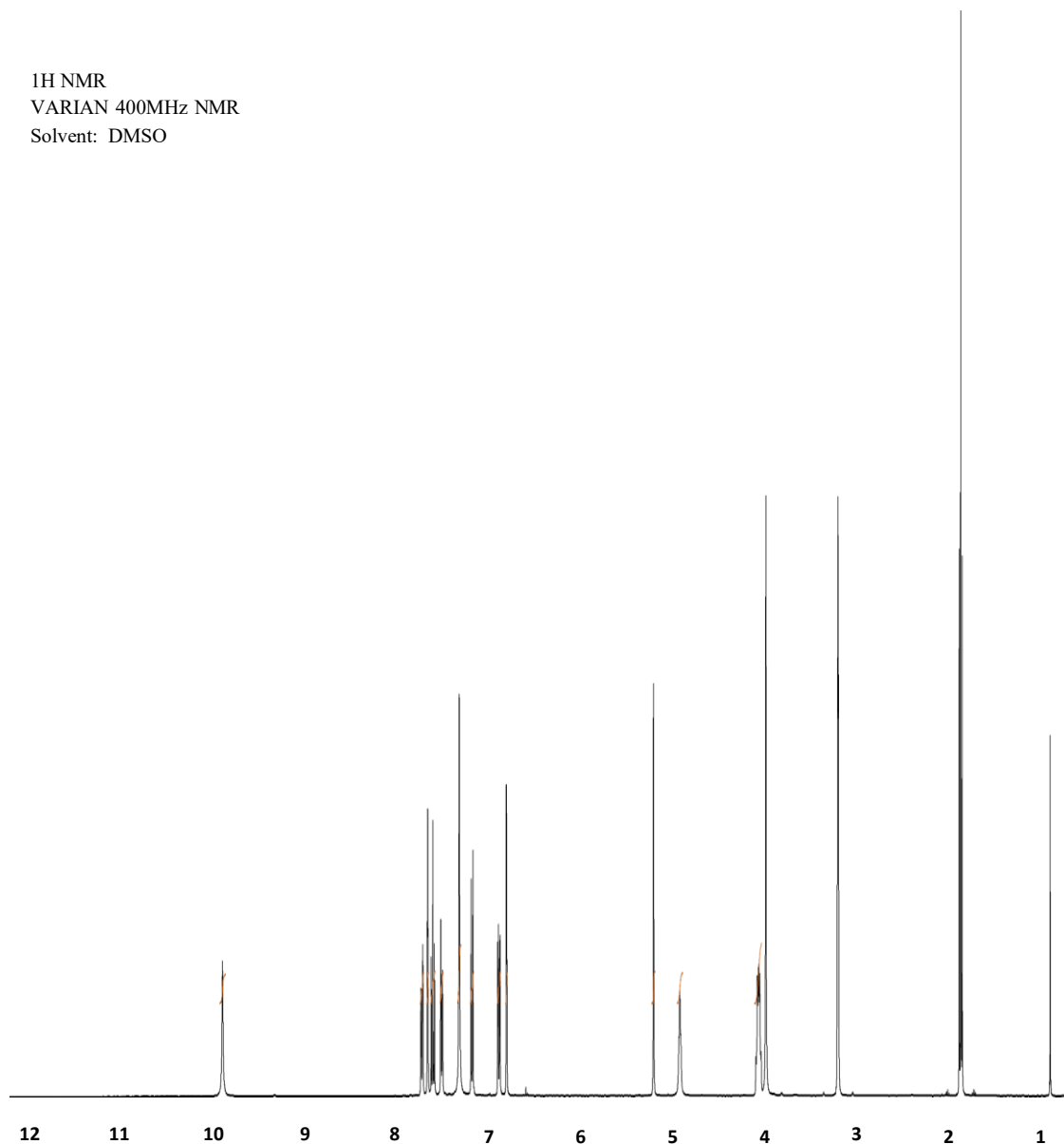
**Graph 2: Graphical representation of MASS Spectroscopy**

❖ NMR Spectroscopy

<sup>1</sup>H NMR (400 MHz, DMSO-d<sub>6</sub>, δ ppm): 9.78 (s, 1H, OH), 7.41 (d, J = 8 Hz, 1H, Ar-H), 7.34 (s, 1H, Ar-H), 7.28 (t, J = 8 Hz, 1H, Ar-H), 7.18 (d, J = 8 Hz, 1H, Ar-H), 6.96 (s, 2H, NH<sub>2</sub>), 6.82 (d, J = 8.4 Hz, 1H, Ar-H), 6.50 (dd, J = 2.4, 8.8 Hz, 1H, Ar-H), 6.41 (d, J = 2.4 Hz, 1H, Ar-H), 4.67 (s, 1H, CH)

The spectrum shows a downfield singlet around 9.8–10 ppm, which corresponds to the phenolic –OH proton. A set of multiple signals between 6.5–7.8 ppm represents the aromatic protons of the benzene ring present in the chromene structure. A distinct signal around 4.5–5.0 ppm is assigned to the methine proton (–CH) at the C-4 position of the chromene ring. A signal near 3.4 ppm corresponds to residual water in DMSO and the peak at 2.5 ppm is due to the DMSO-d<sub>6</sub> solvent signal. Additional upfield signals may correspond to alkyl substituents such as methyl groups in the molecule.

<sup>1</sup>H NMR  
VARIAN 400MHz NMR  
Solvent: DMSO



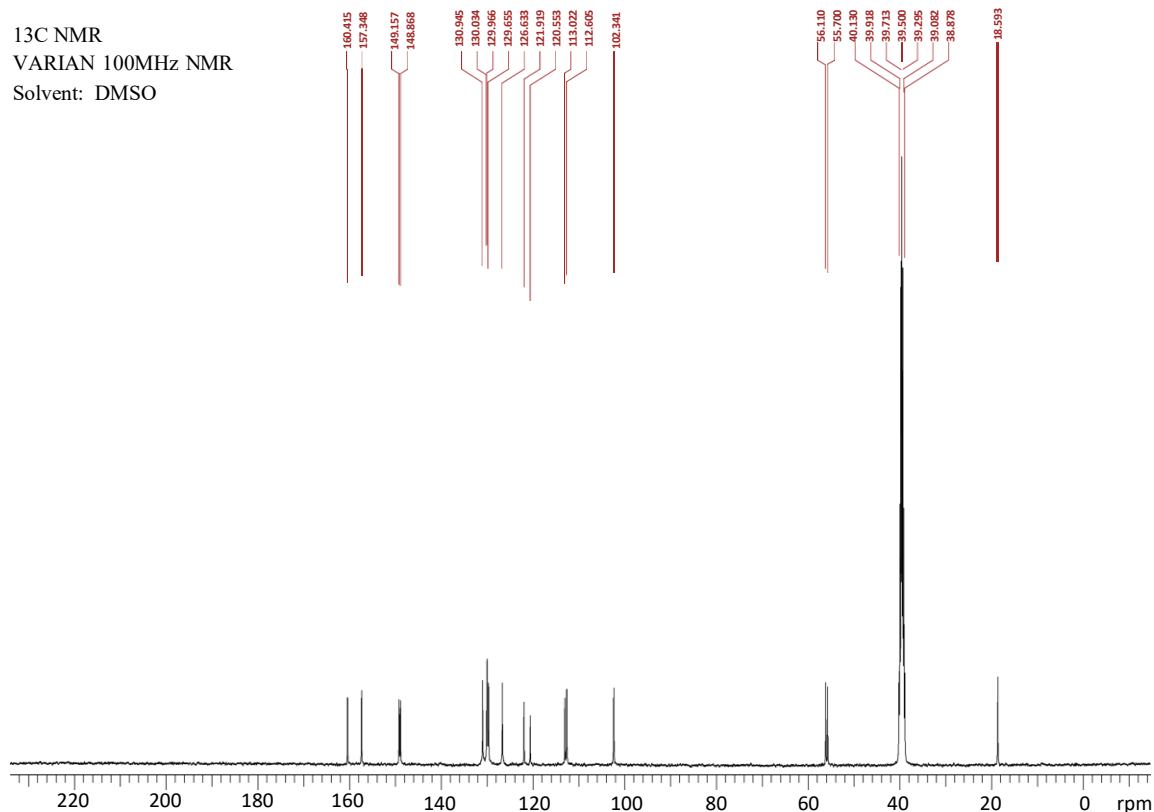
**Graph 3: Graphical representation of <sup>1</sup>H NMR Spectroscopy**

<sup>13</sup>C NMR:

<sup>13</sup>C NMR (DMSO, 100 MHz)  $\delta$  160.415, 157.348, 149.157, 148.868, 130.945, 130.034, 129.966, 129.655, 126.633, 121.919, 120.553, 113.022, 112.605, 102.341, 56.110, 55.700, 40.130, 39.918, 39.713, 39.500, 39.295, 39.082, 38.878.

The signals at 160.415 and 157.346 ppm are assigned to C-OH and C-O carbons of the Chromene ring. Peaks at 149.157–148.868 ppm correspond to quaternary aromatic carbons attached to oxygen. The cluster of signals between 130.945–120.553 ppm are due to carbon attached in phenyl ring and Chromene fused ring. The peak at 113.022 ppm are due to carbon attached in NH<sub>2</sub> group.

The peak at 102.341 are corresponds to carbon attached in CN group. In the aliphatic region, peaks at 56.110 and 55.700 ppm indicate a oxygenated methine carbon. The strong multiple around 38.878–40.130 ppm corresponds to the DMSO-d<sub>6</sub> solvent signal.



Graph 4: Graphical representation of 13C NMR

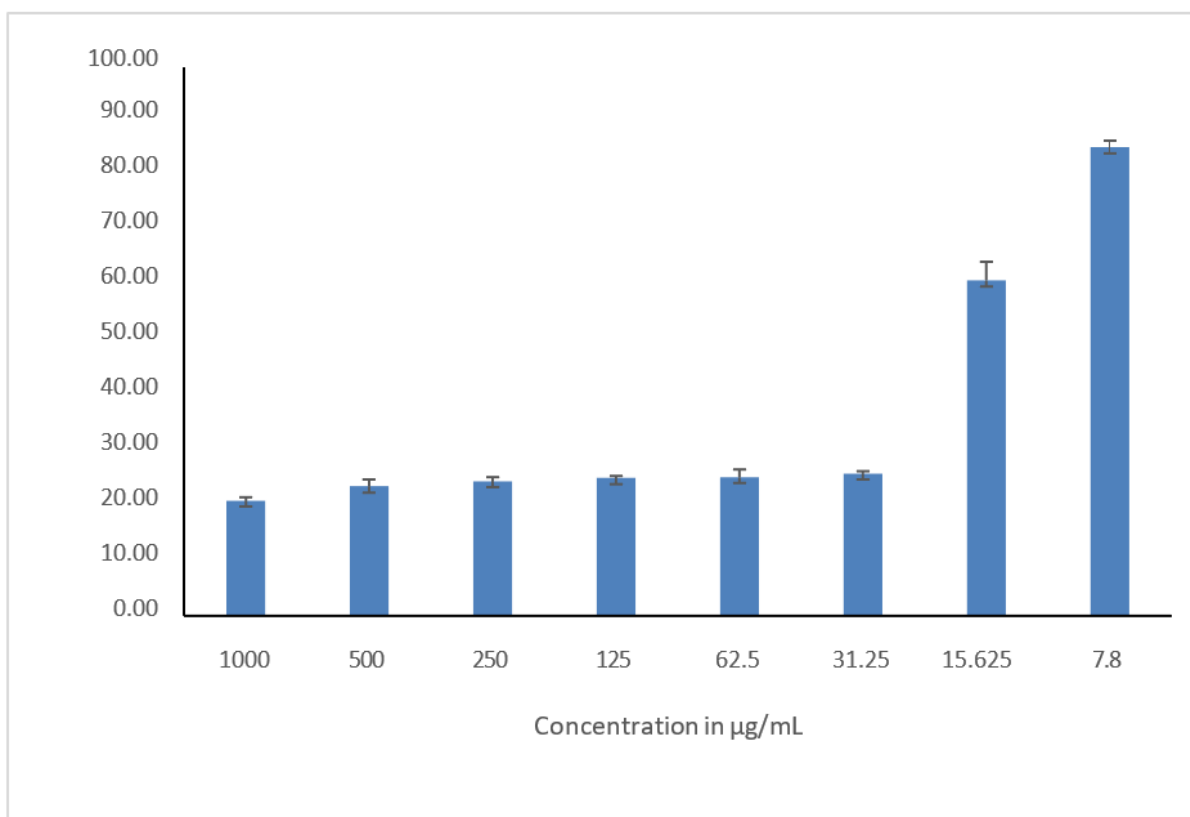
**In-vitro study**

In vitro cytotoxicity of 4H-Chromene Derivative in terms of percentage cell viability against CaCo2 cell line by MTT assay are shown in th table 8.

Concentration (µg/mL)	Percentage of cell Viability (Mean ± SD)	Percentage of cell Cytotoxicity (Mean ±SD)
1000	20.97 ± 0.70	79.03 ± 0.70
500	23.60 ± 1.39	76.40 ± 1.39
250	24.51 ± 0.87	75.49 ± 0.87
125	25.11 ± 0.49	74.89 ± 0.49

62.5	25.26 ± 1.50	74.74 ± 1.50
31.25	25.94 ± 0.46	74.06 ± 0.46
15.625	61.09 ± 3.51	38.91 ± 3.51
7.8	85.37 ± 1.20	14.63 ± 1.20
<b>CTC<sub>50</sub> (µg/mL)</b>	156.97	

**Table 8: Cytotoxicity of 4H-Chromene Derivative in terms of percentage cell viability against CaCo-2 cell line by MTT assay**



**Graph 5: Graphical representation of cytotoxicity in terms of cell viability of 4H-Chromene Derivative in CaCo-2 cells.**

The MTT assay results demonstrate that the 4H-Chromene derivative exhibits a clear dose-dependent cytotoxic effect against the CaCo-2 cell line. At higher concentrations (62.5–1000 µg/mL), the compound markedly reduced cell viability to around 21–26%, corresponding to high cytotoxicity (74–79%). In contrast, lower concentrations showed significantly higher cell viability, with minimal cytotoxic effects observed at 7.8 µg/mL. The calculated CTC<sub>50</sub> value of 156.97 µg/mL indicates moderate cytotoxic potency. Overall, these findings suggest that the 4H-Chromene derivative possesses significant anticancer potential against colorectal

cancer cells. Based on the study results, the compound C4 is considered to be toxic against CaCo-2 cells at tested concentrations.

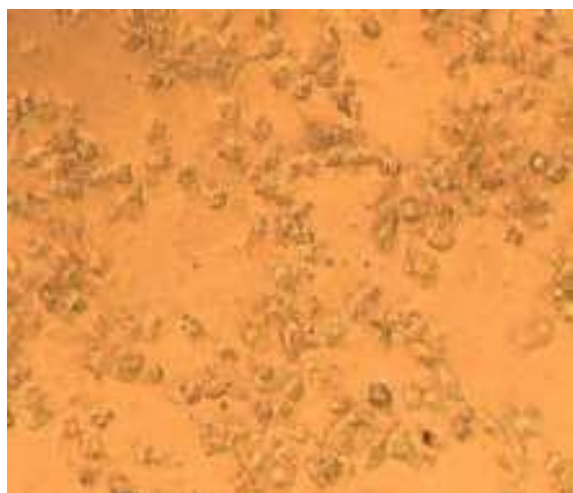


**Figure 13: Morphological change of CaCo2 cell line treatment with 4H-Chromene derivative in 1000 µg/mL**

#### IV. SUMMARY

This study focuses on the discovery of potential anticancer agents based on a series of 4H-Chromene derivatives through an integrated computational and experimental approach. Initially, molecular modeling and docking techniques were applied to design and evaluate the compounds against a cancer-related target protein (EGFR). The designed molecules were further assessed for their binding affinity, drug-likeness, and pharmacokinetic behaviour by using multiple computational tools include Chemskech, GEINFORCE, Force ADME, PyRx and Discovery studio visualizer, enabling the identification of the most promising candidates.

Based on these preliminary findings, selected derivative was synthesized using appropriate organic reaction methods and purified through standard laboratory procedures. The chemical structure and purity of the synthesized compound was confirmed using physicochemical and spectroscopic characterization techniques, including melting point determination, thin-layer chromatography, infrared spectroscopy, nuclear magnetic resonance spectroscopy ( $^1\text{H}$  NMR &  $^{13}\text{C}$  NMR) and mass spectrometry.

After structural confirmation, the compound was evaluated through biological screening for its *in-vitro* anticancer activity against colorectal cancer using the CaCo2 cell line. The results provided insight into the relationship between structural features and biological activity, helping to identify derivatives with improved anticancer potential.

Overall, the study demonstrates that combining computational drug design, chemical synthesis, and biological evaluation is an effective strategy for identifying potential anticancer agents.

#### V. CONCLUSION

4H-Chromene is a biologically significant scaffold known for its diverse pharmacological properties. The present study was designed to investigate the anticancer potential of 4-phenyl-4H-Chromene derivatives with specific emphasis on colorectal cancer. Initially, all designed analogues were subjected to *in-silico* molecular modeling studies against selected cancer-related target (EGFR) to evaluate their binding interactions and inhibitory potential. The derivatives exhibited favourable interaction profiles with the selected target protein. Drug-likeness and toxicity prediction studies further suggested acceptable pharmacokinetic properties and the potential for oral bioavailability. Among these 4-phenyl-4H-Chromene derivatives, C4 exhibited the highest docking score compared to the other derivatives.

Based on the computational findings, the most promising derivative, C4 was synthesized using a conventional one-pot three-component reaction involving Knoevenagel condensation followed by Michael addition, yielding the desired compounds in good amounts. The synthesized compound was purified and structurally confirmed using analytical and spectroscopic techniques such as IR, mass spectrometry, and  $^1\text{H}$  and  $^{13}\text{C}$  NMR analysis.

The synthesised compound was subsequently evaluated for its *in-vitro* anticancer activity against the CaCo2 cell line, a well-established model for colorectal cancer. The biological screening revealed that the compound exhibited significant cytotoxic activity against colorectal cancer cells. Structure-activity relationship analysis indicated that specific substituents, such as electron-donating groups at the 7th position and electronegative halogens at the 3' position of the chromene ring, enhanced anticancer activity.

Overall, the study demonstrates that the 4-phenyl-4H-Chromene derivatives possesses promising potential as a colorectal anticancer agent. The combined approach of computational drug design, chemical synthesis, and *in-vitro* evaluation using CaCo2 cell line provides an effective strategy for identifying a potential new therapeutic agent for colorectal cancer.

## REFERENCES

- [1]. J. Zamocka, E. Misikova, J. Durinda, Cesk-Farm (Ceska a Slovenska Farm-acie) 41 (1992) 170; Chem. Abstr. 116 (1992) 106031.
- [2]. L. Alvey, S. Prado, V. Huteau, B. Saint-Joanis, S. Michel, M. Koch, S.T. Cole, F. Tillequin, Y.L. Janin, Bioorg. Med. Chem. 16 (2008) 8264.
- [3]. T. Narender, Shweta, S. Gupta, Bioorg. Med. Chem. Lett. 14 (2009) 3913.
- [4]. S.J. Mohr, M.A. Chirigos, F.S. Fuhrman, J.W. Pryer, Cancer Res. 35 (1975) 3750.
- [5]. V.K. Tandon, M. Vaish, S. Jain, D.S. Bhakuni, R.C. Srimal, Indian J. Pharm. Sci. 53(1991) 22.
- [6]. M. Brunavs, C.P. Dell, P.T. Gallagher, W.M. Owton and C.M. Smith, European Pat. Appl. EP. 557, 075 (1993). Chem. Abstr. 120 (1994) 106768.
- [7]. M. Longobardi, A. Bargagna, E. Mariani, P. Schenone, E. Marmo, IL Farmaco 45(1990) 399.
- [8]. T. Narender, Shweta, S. Gupta, K. Gortlitz, A. Dehre, E. Engler, Arch. Pharm. Weinheim Ger. 316 (1983) 264.
- [9]. P. Coudert, J.M. Coyquelet, J. Bastide, Y. Marion, J. Fialip, Ann. Pharm. Fr. 46(1988) 91.
- [10]. F. Eiden, F. Denk, Arch. Pharm. Weinheim Ger. 324 (1991) 875.
- [11]. C. Bruhlmann, F. Ooms, P. Carrupt, B. Testa, M. Catto, F. Leonetti, C. Altomare, A. Cartti, J. Med. Chem. 44 (2001) 3195.
- [12]. S.R. Kesten, T.G. Heffner, S.J. Johnson, T.A. Pugsley, J.L. Wright, D.L. Wise, J. Med. Chem. 42 (1999) 3718.
- [13]. A. Bargagna, M. Longobardi, E. Mariani, P. Schenone, E. Marmo, IL Farmaco 45(1990) 405.
- [14]. A. Bargagna, M. Longobardi, E. Mariani, P. Schenone, E. Marmo, IL Farmaco 46(1991) 461.
- [15]. A. Bargagna, M. Longobardi, E. Mariani, P. Schenone, C. Falzarano, IL Farmaco 47 (1992) 345.
- [16]. K. Gortlitz, A. Dehre, E. Engler, Arch. Pharm. Weinheim Ger. 317 (1984) 526.
- [17]. A. Ermili, G. Roma, M. Buonamici, A. Cuttica, M. Galante, IL Farmaco 34 (1979) 535.
- [18]. W.P. Smith, L.S. Sollis, D.P. Howes, C.P. Cherry, D.I. Starkey, N.K. Cobley, J. Med. Chem. 41 (1998) 787.
- [19]. R.N. Taylor, A. Cleasby, O. Singh, T. Sharzynski, J.A. Wonacott, W.P. Smith, L.S. Sollis, D.P. Howes, C.P. Cherry, R. Bethell, P. Colman, J. Varghese, J. Med. Chem. 41 (1998) 798.
- [20]. K. Hiramoto, A. Nasuhara, K. Michiloshi, T. Kato, K. Kikugawa, Mutat. Res. 395(1997) 47.
- [21]. A.G. Martinez, L.J. Marco, Bioorg. Med. Chem. Lett. 7 (1997) 3165. 22
- [22]. Kolla, S. R., and Lee, Y. R. (2011). Ca (OH) 2-mediated efficient synthesis of 2-amino-5-hydroxy-4H-chromene derivatives with various substituents. Tetrahedron 67, 8271–8275.
- [23]. Ramesh, R., Vadivel, P., Maheswari, S., and Lalitha, A. (2016). Click and facile access of substituted tetrahydro-4H-chromenes using 2-aminopyridine as a catalyst. Res. Chem. Intermed. 42, 7625–7636.
- [24]. Marini H., Minutoli L., Polito F., Bitto A., Altavilla D., Atteritano M., (2007). Effects of the Phytoestrogen Genistein on Bone Metabolism in Osteopenic Postmenopausal Women: a Randomized Trial. Ann. Intern. Med. 146 (12), 839–847.
- [25]. Dixon R., Ferreira D. (2002). Genistein. Phytochemistry 60 (3), 205–211.
- [26]. Zhixiong Zhang, Chengdi Wang. Molecular mechanism of colibulin in complex with tubulin provides a rationale for drug design, 2 April 2019.
- [27]. Gopal Menon; Burt Cagir. Colon Cancer. National Library of Medicine. February 27, 2025.
- [28]. Worthley DL, Leggett BA. Colorectal cancer: molecular features and clinical opportunities. Clin Biochem Rev. 2010 May;31(2):31-8.
- [29]. Mármol I, Sánchez-de-Diego C, Pradilla Dieste A, Cerrada E, Rodríguez Yoldi MJ. Colorectal Carcinoma: A General Overview and Future Perspectives in Colorectal Cancer. Int J Mol Sci. 2017 Jan 19;18(1).
- [30]. Huang J, Soupir AC, Schlick BD, Teng M, Sahin IH, Permeth JB, Siegel EM, Manley BJ, Pellini B, Wang L. Cancer Detection and Classification by CpG Island Hypermethylation Signatures in Plasma Cell-Free DNA. Cancers (Basel). 2021 Nov 09;13(22).
- [31]. Guinney J, Dienstmann R, Wang X, de Reyniès A, Schlicker A, Soneson C, Marisa L, Roepman P, Nyamundanda G, Angelino P, Bot BM, Morris JS, Simon IM, Gerster S, Fessler E, De Sousa E Melo F, Missiaglia E, Ramay H, Barras D, Homicsko K, Maru D,

- Manyam GC, Broom B, Boige V, Perez-Villamil B, Laderas T, Salazar R, Gray JW, Hanahan D, Taberero J, Bernardis R, Friend SH, Laurent-Puig P, Medema JP, Sadanandam A, Wessels L, Delorenzi M, Kopetz S, Vermeulen L, Tejpar S. The consensus molecular subtypes of colorectal cancer. *Nat Med.* 2015 Nov;21(11):1350-6.
- [32]. Kalpana K, Dr. G. N. K. Suresh Babu. Colorectal Cancer Symptoms and Risk Factors - A Review ,18 Nov 2024.
- [33]. Pak, H.; Maghsoudi, L.H.; Soltanian, A.; Gholami, F. Surgical complications in colorectal cancer patients. *Ann. Med. Surg.* 2020, 55, 13–18.
- [34]. Theodorescu, D. Cancer cryotherapy: Evolution and biology. *Rev. Urol.* 2004, 6 (Suppl. S4), S9.
- [35]. Bageacu, S.; Kaczmarek, D.; Lacroix, M.; Dubois, J.; Forest, J.; Porcheron, J. Cryosurgery for resectable and unresectable hepatic metastases from colorectal cancer. *Eur. J. Surg. Oncol.* 2007, 33, 590–596.
- [36]. Potemin, S.; Kübler, J.; Uvarov, I.; Wenz, F.; Giordano, F. Intraoperative radiotherapy as an immediate adjuvant treatment of rectal cancer due to limited access to external-beam radiotherapy. *Radiat. Oncol.* 2020, 15, 11.
- [37]. Longley, D.B.; Harkin, D.P.; Johnston, P.G. 5-fluorouracil: Mechanisms of action and clinical strategies. *Nat. Rev. Cancer* 2003, 3, 330–338.
- [38]. Dvorak, H.F. Vascular permeability factor/vascular endothelial growth factor: A critical cytokine in tumor angiogenesis and a potential target for diagnosis and therapy. *J. Clin. Oncol. Off. J. Am. Soc. Clin. Oncol.* 2002, 20, 4368–4380.
- [39]. The drug development process US Food and Drug Administration, 4 January 2018, Retrieved 18 December 2019.
- [40]. The drug development process: Discover . US Food and Drug Administration. 4 January 2018. Retrieved 18 December 2019.
- [41]. Helleboid S, Haug C, Lamottke K. The Identification of Naturally Occurring Neoruscogenin as a Bioavailable, Potent, and High-Affinity Agonist of the Nuclear Receptor ROR $\alpha$  (NR1F1). *Journal of Biomolecular Screening.* 2014;19(3):399–406.
- [42]. Herrmann, A., Roesner, M., Werner, T. et al. Potent inhibition of HIV replication in primary human cells by novel synthetic polyketides inspired by Aureothin. *Sci Rep* 10, 1326 (2020).
- [43]. The drug development process: Step 3: Clinical research". US Food and Drug Administration. 4 January 2018. Retrieved 18 December 2019.
- [44]. Paul, S.M Mytelka, D.S Dunwiddie, C.T Persinger, C.C Munos et al. How to improve R&D productivity. The pharmaceutical industry's grand challenge. *Nat.Rev. Drug Disco.*2010, 9, 203-214.
- [45]. Morgan, P, Van Der Graaf, P.H, Arrowsmith, Feltner. Fundamental pharmacokinetics and pharmacological principles toward improving phase II survival. *Drug Discov. Today* 2012, 17, 419-424.
- [46]. Bajorath, J. Integration of virtual and high-throughput screening. *Nat. Rev. Drug Discov.*2002, 1, 882- 894. 85.
- [47]. A. Zielesny. Chemistry Software Package ChemOffice Ultra 2005. *Journal of Chemical Information and Modeling* 2005, 45 (5), 1474-1477.
- [48]. Hemming AW, Davis NL, Klufftinger A et al. Prognostic markers of colorectal cancer: an evaluation of DNA content, epidermal growth factor receptor, and Ki-67. *J Surg Oncol* 1992; 51: 147–52.
- [49]. Mayer A, Takimoto M, Fritz E, Schellander G, Kofler K, Ludwig H. The prognostic significance of proliferating cell nuclear antigen, epidermal growth factor receptor, and *mdr* gene expression in colorectal cancer. *Cancer* 1993; 71: 2454–60.
- [50]. Yang JL, Qu XJ, Russell PJ, Goldstein D. Interferon-alpha promotes the anti-proliferative effect of Erlotinib (OSI-774) on human colon cancer cell lines. *Cancer Lett* 2005; 225: 61–74.
- [51]. Alberto Feliciano, Omar Gomez Garcia, Carlos H Escalante, Mario a, Mariana vargas, Alvares Toledano. Three-Component Synthesis of 2-Amino-3-cyano-4H-chromenes, InSilico Analysis of Their Pharmacological Profile, and In Vitro Anticancer and Antifungal Testing. *Pharmaceuticals* 2021, 14, 1110.
- [52]. Townsley CA, Major P, Siu LL et al. Phase II study of erlotinib (OSI-774) in patients with metastatic colorectal cancer. *Br J Cancer* 2006; 94: 1136–43.
- [53]. Silverstein, R. M., Webster, F. X., Kiemle, D. J., & Bryce, D. L. John Wiley & Sons. *Introduction to Spectroscopy.* 8th Edition, 2014.



- [54]. Claridge, T. D. W. Elsevier. Understanding NMR Spectroscopy 3rd Edition, 2016.
- [55]. McLafferty, F. W., & Tureček, F. University Science Books. Mass Spectrometry: Principles and Applications 4th Edition, 1993.
- [56]. Scudiero DA, Shoemaker RH, Paull KD, Monks A, Tierney S, Nofziger TH, Currens MJ, Seniff D, Boyd MR. Evaluation of a soluble tetrazolium/formazan assay for cell growth and drug sensitivity in culture using human and other tumor cell lines. *Cancer Research*. 1988 Sep 1;48 (17): 4827-33.